Title: Deep learning prediction of material properties

Authors : Charles Le Losq[1,2,3,*], Andrew Valentine[2], Bjorn O. Mysen[3], Daniel R. Neuville[1]

Affiliations :

[1]Institut de physique du globe de Paris, Université de Paris, Paris 75005, France

[2] Research School of Earth Sciences, Australian National University, Canberra 2601, Australia

[3] Geophysical Laboratory, Carnegie Institution for Science, Washington D.C. 20001, U.S.A.

*Correspondence to: lelosq@ipgp.fr

We want to dedicate this manuscript to the memory of G.N. Greaves, which sadly passed away this year. His contributions to the field of material and glass sciences will be remembered.

Abstract: (121/125 w)

Knowledge of the tryptic relationship between chemical composition, molecular structure and macroscopic properties of materials like minerals or glasses is fundamental in many disciplines, including metallurgy, Earth and material sciences. Several avenues allow prediction of this relationship, but usually this task remains very challenging. Deep learning represents a new tool to perform such task, allowing one to link experimental results, models, and even different theories. Focusing on alkali aluminosilicate melts, of prime importance for volcanology and glass sciences, we show how a deep neural network leverages experimental data and theoretical knowledge for prediction of melt and glass properties, including viscosity, fragility, density, or even glass Raman signals. Such approach provides a new, exciting way to build models for various applications.

One sentence summary (96/125 characters): Deep learning bridges the gap between data and models for practical material property prediction

Main Text:

Prediction of the properties of materials is not only fundamental for material engineering and manufacturing, but allows addressing key questions in the areas of physics, chemistry and geosciences. Such predictions rely on understanding and modeling the links between material properties, chemical composition and atomic/ionic structure. The usual approaches consist in getting observations from experiments or from thermodynamic or molecular dynamics (MD) simulation models, and in some case in combining both if possible (e.g. *1, 2*). CALPHAD calculations (*3*) and MD simulation (*4*) have been successful at predicting properties of simple materials like binary alloys or at specific conditions (e.g. very high temperatures in MD), but they are not yet ready for prediction of the properties of complex materials like oxide glasses and minerals at pressures and temperatures pertinent for industry or Earth sciences. Thermodynamic models often offer an intermediate way of predicting macroscopic properties, but the experimentalist still has to link thermodynamic variables to data, and this often turns out to be challenging. In such context, machine learning can represent a “middle man”, allowing scientists to make sense of their data and to put them in the context of different models and theories.

Machine learning is often used for supervised classification or regression tasks, linking independent variables X (e.g. images or x values of a function $y = f(x)$...) to observations Y (e.g. image labels or target values y). Due to its recent democratization, many software frameworks exit to perform such tasks. Particularly, an exciting development is that those frameworks allow one to track gradients in any differentiable models via automatic differentiation. We can use such ability for training models combining machine learning parts, like artificial neural networks, with physical / thermodynamic equations by gradient descent. An ideal case for the application of this

approach lies in prediction of the link between chemical composition, structure and properties of aluminosilicate melts and glasses (e.g., see the review of [5]). First, those materials are critical for Earth and material sciences: they form the liquid part of magmas, which viscosity directly drives the effusive or explosive dynamic of volcanic eruptions ([6]), and, as glasses, they are so important nowadays that we probably are living in the Glass Age ([7]). Secondly, different theories link the structure of those liquids to their properties, and involve variables that are either difficult or impossible to measure directly, like glass configurational entropy S^{conf}. In this publication, we show how the combination of a deep neural network with different equations allows linking composition, thermodynamic and structural variables for such materials. For simplicity, we focused on compositions in the K_2O-Na_2O-Al_2O_3-SiO_2 system, as it starts to be well know with a quite complete (but still fairly sparse!) dataset (Fig. S1).

The deep neural network takes the composition of the melts/glasses in input (Fig. 1), and predicts various properties of glasses like density, optical refractive index and Raman spectra, as well as melt thermodynamic and structural variables like glass transition temperature T_g, configurational entropy S^{conf} ([8, 9]) or fragility m ([10]). The network was trained using four viscosity ($D_{viscosity}$), density ($D_{density}$), optical refractive index ($D_{optical}$) and Raman spectra (D_{Raman}) datasets; each dataset was split in *training*, *validation* and *testing* subsets (except D_{raman} only split in *training* and *validation* subsets due to its very small size), the *testing* one being unseen during training and used to test the model predictive ability. Experiments were performed to complete some parts of the quaternary diagram where data were too scarse (see Supplementary Materials and Methods and Tables S1-2). Multitask learning combined with early-stopping, dropout and bagging allowed promoting the model predictive (a.k.a. generalization) ability despite the use of

small datasets for training (Supplementary Material and Methods). In the following, we first show how the model allows trans-theoretical predictions of melt viscosity. We then see how thermodynamic and structural parameters can be predicted, and how this can be leveraged to link different theories or to investigate if Raman spectra could be used for material property predictions.

Results

Trans-theoretical predictions: example of melt viscosity

There is a vast landscape of theories (and their associated set of equations) describing the viscous flow of liquids, supported by different arguments depending on usecase (e.g. *11*). Trans-theoretical modeling, i.e. the ability to simultaneously use equations from different theories in the same model, may solve such problem as it allows unbiased comparison of results on the same dataset. In this work, we tested different theories and equations proposed to describe the viscous flow of aluminosilicate melts, like the Adam and Gibbs (AG) (*8*) and the free volume (FV) (*12*) theories, respectively proposing the following equations to decribe viscous flow of melts:

$$\log \eta(T,x) = A_e(x) + \frac{B_e(x)}{T\left(S^{conf}(T_g,x) + \int_{T_g}^{T} C_p^{conf}(x)/T\,dT\right)}, \quad (1)$$

and

$$\log \eta(T,x) = A_{FV}(x) + 2\,B_{FV}(x) / \left(T - T_o(x) + \sqrt{\left((T - T_o(x)\right)^2 + C_{FV}(x)T}\right), \quad (2)$$

where x is the melt composition, A_e and A_{FV} are pre-exponential terms proportional to $\log \eta(T \longrightarrow \infty)$, B_e is a constant proportional to the energy barriers opposed to the cooperative molecular re-arrangements of melt structure upon viscous flow, S^{conf} and C_p^{conf} are the melt

configurational entropy and heat capacity, T_g is the melt glass transition temperature, and B_{CG}, C_{FV} and T_0 are parameters linked to the distribution of free volumes in the liquids in the FV theory. The AG theory assumes that viscous flow is related to entropic effects resulting from cooperative rearrangement of molecular subunits, while the FV theory states that viscous flow occurs through cooperative exchanges of free volumes within the liquid. The AG model is usually preferred for silicate melts (*9*, *13*, *11*, *14*), but one could always question if other models may not be also appropriate (Supplementary Text).

After training (see details in Supplementary Text), the model allows systematic predictions of melt viscosity using the Adam-Gibbs theory, as shown in Figure 2A where model predictions and measurements are compared for melts with ~66 mol% SiO_2 and varying Al/(Na+K) and K(K+Na). Other theories can also be used, like the FV theory that yields a precision similar to the AG theory (Fig. 2B,C). Semi-empirical and empirical equations, like the famous Tamman-Vogel-Fulcher equation, yield a good precision too (Supplementary Text and Figure S3). In all cases, predictive errors are lower than 0.50 log Pa·s, as shown by root-mean-square-errors (RMSE) ~ 0.45 log Pa·s on the *testing* data subset (Table S3). Errors are slightly higher in the supercooled domain (viscosity > 10^7 Pa·s) for all theories (Fig. S3) because, in this domain, melt entropy (eq. 1) varies in a complex manner depending on melt composition (see discussion) and this results in large, non-linear viscosity variations difficult to reproduce. Interestingly, based on only numerical performance, the different viscosity models yield similar precisions (Table S3 and Figure S3) and it may seem difficult to discriminate a better one (Fig. 2B,C; see also Table S3). However, the AG theory relates measurable thermodynamic variables to melt viscosity (*9*) and performs as well as, or better than others equations. Consequently, present results confirm that this theory seems well appropriate for aluminosilicate melts. Aside this and more generally,

the obtained results clearly indicate that deep learning allows practical trans-theoretical modeling, a feature extremely interesting in many areas.

Thermodynamic and static property predictions

Beyond trans-theoretical viscosity predictions, the present model offers the possibility to predict aluminosilicate melt thermodynamic properties: known viscous T_g *and* $S^{conf}(T_g)$ are predicted within 16 K and 0.8 J mol^{-1} K^{-1}, respectively (RMSE on testing subsets; Fig. S4). Glass properties are also successfully predicted, as shown by RMSE on testing density and refractive index data subsets of 0.009 g cm^{-3} and 0.005, respectively. Confident in the model predictive ability, we can now use it to explore how parameters like $S^{conf}(T_g)$, a driver of melt rheology (eq. 1), vary with melt composition in the entire glass-forming domain of the Na_2O-K_2O-Al_2O_3-SiO_2 diagram.

Variations in $S^{conf}(T_g)$ with melt composition are non-monotonic, with maxima close to, or on the silicate joint (alkali-silica, Al-free), while in general a decrease in $S^{conf}(T_g)$ is observed upon addition of aluminum (Fig. 3A,B). Increasing the fraction of $MAlO_2$ (M=Na, K) decreases $S^{conf}(T_g)$, the effect being more linear and pronounced for potassic compositions (Fig. 3B). Mixing alkalis result in different effects as a function of the M/Al ratio of the melt (Fig. 3C,D). For silicate compositions, the Mixed Alkali Effect (MAE) (*15*) is observed: a maximum in $S^{conf}(T_g)$ is generally observed as Na and K mix, except at very low (< 0.55) or very high (> 0.95) silicate contents. At high Al concentrations, the variations in entropy with the Na/K ratio are closer to a linear trend, indicating a different MAE (*2*).

Similarly to melt entropy, the melt glass transition temperature T_g vary largely as a function of melt composition (Fig. 4A,B). This allows large changes in melt dynamic properties with only limited variations in fragility (Fig. S6). We finally note that variations in glass density and refractive index with composition are also smooth and monotonic, both parameters depending mostly on the glass SiO_2 fraction, and in lesser extents on its M/Al as well as Na/K ratios (Fig. 4C,D,E,F). Those parameters are actually correlated between themselves, as visible in corner plots (see supplementary Jupyter Notebooks).

Raman spectra: a glimpse into melt structure

Raman spectra were used as a way to perform multitask learning (Supplementary Text) and to introduce structural information in the artificial neural network. The dataset we have is limited (48 compositions), such that we did not aim at having excellent predictions, but we simply wanted the network to capture the general Raman signal variations as a function of glass composition. This goal is achieved: predicted and measured R_{Raman}, the ratio between signals assigned to intertetrahedral vibrations (below 670 cm^{-1}) and intratetrahedral vibrations (between ~860 and 1300 cm^{-1}) compare well (Fig. 5A), and the median of the relative mean absolute deviation between predicted and measured Raman spectra (Fig. S7) is of 22 % on the validation D_{Raman} subset. The model thus captured the general link between glass composition and glass structure as sampled by Raman spectroscopy, but remains affected by some evident predictive errors (Fig. S7), particularly at high silica concentrations where the dataset is particularly scares (Fig. S1). Better results could be obtained by improving the coverage of the Raman spectral database in the future.

Discussion

The developed framework offers unique opportunities to objectively explore the links between chemical, structural, thermodynamic and dynamic parameters in materials. Such task is traditionally done by humans, and this situation is far from being ideal as we are influenced by various biases (*16*). For example, because of the known link between melt structure and properties, one can propose that melt viscosity could be predicted solely from R_{Raman} (*17*), with the benefit that this value is measured via a cheap, rapid to perform, non-damaging, spatially-resolved spectroscopy that can be easily deployed *in situ*. However, this is forgetting the importance of ionic mixing effects on the thermodynamic properties of melts (*15, 9, 13*). Indeed, Raman spectra are only a spectroscopic picture of the AlO_4-SiO_4 polyhedral network topology, which is barely affected by ionic mixing effects (*18*). Therefore, it should not be possible to predict melt viscosity from only Raman spectra. Our results confirm this: in the investigated system, while there is a general non-linear correlation between R_{Raman} and T_g for instance (Fig. 5B; Spearman correlation coefficient r_s = 0.98), $S^{conf}(T_g)$ and melt fragility m display complex variations with R_{Raman} (Fig. 5C,D). Such complexity further explains why no general model of $S^{conf}(T_g)$ or m has been proposed to date.

The trans-theoretical character of the model allows adopting a new vision about a problem like melt viscous flow and glass transition. For aluminosilicate melts, it allows observing the link between two theories: Adam-Gibbs (AG) and Free Volume (FV). In the FV theory, solid-like and liquid-like molecular cells are distinguished and separated by a critical volume v^*, and viscous flow occurs via cooperative molecular movements between liquid-like cells. In the AG theory, viscous flow occurs via cooperative motions of molecular segments of a size $z^*(T)$,

characterized by an intrisic entropy S_c^*. The two theories thus share some common philosophical background: viscous flow is assumed to occur via some sort of cooperative movements of molecular entities in the melt. This background can be retrieved when diving into the details of the parameters of eq. 1 and 2. Indeed, B_{CG} embeds some structural information because it depends on v^*:

$$B_{CG} = v^* z_o, \quad (5)$$

where z_o is an adjustable parameter. Similarly, the ratio $B_e/S^{conf}(T_g)$ embeds molecular subunits lengthscale information as

$$B_e/S^{conf}(T_g) = [\ \Delta\mu\ z^*(T_g)\ ] / R, \quad (6)$$

with $\Delta\mu$ the energy barriers opposed to the rearrangement of molecular subunits of size $z^*(T_g)$, and R the perfect gas constant. Now let's consider v^* and z^* as structural parameters embedding information about the volume or lengthscale of cooperative molecular regions. In this case, they should directly depend on melt or glass structure. This is confirmed by the fact that both B_{CG} and $B_e/S^{conf}(T_g)$ correlate very well with R_{Raman} (Fig. 5E,F, r_s = 0.987 and 0.985 respectively), which provides information about the network connectivity; the higher R_{Raman} is, the higher the interconnection between polyhedral units, thus the higher the 3D network topology (*19*). In detail, this implies that it actually should be possible to develop a free-volume version of the AG theory, as it has been proposed (*20*, *21*). More generally, the links between B_{CG}, $B_e/S^{conf}(T_g)$ and R_{Raman} support the hypothesis that melt viscous flow occurs when a critical molecular lengthscale is reached. This lengthscale can be determined from Raman spectra (Fig. 5E,F) and strongly influences the glass transition temperature T_g (Fig. 5B). In detail, entropic effects (like the excess of entropy resulting from the MAE) also affect T_g (*18* and references cited therein) but their influence remains limited compared to that of the polyhedral network topology (Fig. 5B). On the

other hand, such entropic effects strongly control the rate at which supercooled melt viscosity changes as a function of T, or in other terms, the melt fragility *m* because $m \propto C_p^{conf} / S^{conf}\left(T_g\right)$ (Fig. S5). Actually, we may consider that such mixing phenomena are allowed by the non-ergotic nature of melts, their inhomogeneities being frozen into glasses below T_g. Following from this idea, it is possible to relate *m* to ongoing density fluctuations inherited from dynamic heterogeneities formed at supercooled T, i.e. $T_{liquidus} < T < T_g$ (*22*). The nature of such heterogeneities is expected to change largely with melt composition, as we can recognize different cases for network organization as described by the Random Network for simple AX_2 glasses like SiO_2 (*23*), the Modified Random Network for silicate liquids (*24*) and the Continuous Compensated Random Network (*25*, *2*) for aluminum-rich aluminosilicates, each one presenting distinct and different extent of heterogeneities at medium and long range order with various associated cationic mixing within such heterogeneities that drive large and complex changes in glass configurational entropy (Supplementary Text) and hence viscosity (Fig. 2A).

The presented approach is flexible, improvable, and transposable. The present model, which successfully links chemistry, structure and properties of aluminosilicate melts and glasses, is a proof a concept, and is meant to change and evolve in the future. Different improvements will consist in, for instance, (i) extending it to compositions containing cations like Ca, Mg, Ti or Fe, (ii) including other equations to predict melt viscosity, or (iii) adding other spectroscopic information like ^{29}Si and ^{27}Al nuclear magnetic resonance spectra. At the moment, the principal limitation of the model resides in the limited sets of experimental data available for training. The combination of different methods (early stopping, dropout, multitask learning, bagging) allowed successful training of the model on small datasets, but a significant number of compositions are

still needed to obtain good results (more than 80 in the present case, see Supplementary Text and Fig. S2). This may represent a problem for including compositions for which available data are very sparse, like aluminate melts. In addition, entropy variations due to mixing of different alkali and alkaline-earth cations (e.g., Ca-K, Mg-K…) remain not well known, and this may be another difficulty to solve in the future. Despite such potential problems, and considering existing data on simple melts as well as geologic compositions, extension of the present model to compositions pertinent for geologic and industrial melts is realistic. More importantly, the present approach can be readily transposed to other problems in the fields of chemistry, physics, geo- and material sciences where only part of the problem can be solved via know equations, and other parts linking many different observations on an object like a material or a system are fully unknown but can be learn from data using deep learning. The present work proves that this is possible on small datasets, and can bring invaluable information about long-standing problems.

References and Notes. (40 citations max main text)

1. .....Y. Wang, T. Sakamaki, L. B. Skinner, Z. Jing, T. Yu, Y. Kono, C. Park, G. Shen, M. L. Rivers, S. R. Sutton, Atomistic insight into viscosity and density of silicate melts under pressure. *Nat. Commun.* **5** (2014), doi:10.1038/ncomms4241.

2. .....C. Le Losq, D. R. Neuville, W. Chen, P. Florian, D. Massiot, Z. Zhou, G. N. Greaves, Percolation channels: a universal idea to describe the atomic structure and dynamics of glasses and melts. *Sci. Rep.* **7**, 16490 (2017).

3. .....N. Saunders, A. Miodownik, *CALPHAD (calculation of phase diagrams): a comprehensive guide* (Elsevier., 1998).

4. .....D. C. Rapaport, *The art of molecular dynamics simulation* (Cambridge University Press, Cambridge, U.K., ed. 2nd, 2004).

5. .....C. Le Losq, M. R. Cicconi, G. N. Greaves, D. R. Neuville, in *Handbook of Glass* (Springer, 2019; https://www.springer.com/us/book/9783319937267).

6. .....D. B. Dingwell, Volcanic Dilemma - Flow or Blow? *Science*. **273**, 1054–1055 (1996).

7. .....D. L. Morse, J. W. Evenson, Welcome to the Glass Age. *Int. J. Appl. Glass Sci.* **7**, 409–412 (2016).

8. .....G. Adam, J. H. Gibbs, On the temperature dependence of cooperative relaxation properties in glass-forming liquids. *J. Chem. Phys.* **43**, 139–146 (1965).

9. .....P. Richet, Viscosity and configurational entropy of silicate melts. *Geochim. Cosmochim. Acta*. **48**, 471–483 (1984).

10. . .C. A. Angell, Relaxation in liquids, polymers and plastic crystals—strong/fragile patterns and problems. *J. Non-Cryst. Solids*. **131**, 13–31 (1991).

11. .....Y. Bottinga, P. Richet, A. Sipp, Viscosity regimes of homogeneous silicate melts. *Am. Mineral.* **80**, 305–318 (1995).

12. .....M. H. Cohen, G. S. Grest, Liquid-glass transition, a free-volume approach. *Phys. Rev. B.* **20**, 1077 (1979).

13. .....D. R. Neuville, P. Richet, Viscosity and mixing in molten (Ca, Mg) pyroxenes and garnets. *Geochim. Cosmochim. Acta*. **55**, 1011–1019 (1991).

14. ..P. Richet, Residual and configurational entropy: Quantitative checks through applications of Adam-Gibbs theory to the viscosity of silicate melts. *J. Non-Cryst. Solids*. **355**, 628–635 (2009).

15. .....D. E. Day, Mixed alkali glasses - Their properties and uses. *J. Non-Cryst. Solids*. **21**, 343–372 (1976).

16. .....T. J. Kaptchuk, Effect of interpretive bias on research evidence. *BMJ*. **326**, 1453–1455 (2003).

17. .....D. Giordano, J. K. Russell, Towards a structural model for the viscosity of geological melts. *Earth Planet. Sci. Lett.* **501**, 202–212 (2018).

18. .....C. Le Losq, D. R. Neuville, Molecular structure, configurational entropy and viscosity of silicate melts: Link through the Adam and Gibbs theory of viscous flow. *J. Non-Cryst. Solids*. **463**, 175–188 (2017).

19. ....G. N. Greaves, A. L. Greer, R. S. Lakes, T. Rouxel, Poisson's ratio and modern materials. *Nat. Mater.* **10**, 823–837 (2011).

20. .....I. M. Hodge, Enthalpy relaxation and recovery in amorphous materials. *J. Non-Cryst. Solids*. **169**, 211–266 (1994).

21. .....G. Liu, D. Zhao, Y. Zuo, Modified Adam–Gibbs models based on free volume concept and their application in the enthalpy relaxation of glassy polystyrene. *J. Non-Cryst. Solids*. **417**–**418**, 52–59 (2015).

22. .....H. Shintani, H. Tanaka, Frustration on the way to crystallization in glass. *Nat. Phys.* **2**, 200–206 (2006).

23. .....W. H. Zachariasen, The atomic arrangement in glass. *J. Am. Chem. Soc.* **54**, 3841–3851 (1932).

24. .....G. N. Greaves, Exafs and the structure of glass. *J. Non-Cryst. Solids*. **71**, 203–217 (1985).

25. .....G. N. Greaves, K. L. Ngai, Reconciling ionic-transport properties with atomic structure in oxide glasses. *Phys. Rev. B*. **52**, 6358–6380 (1995).

Supplementary Material References

To be done prior to submission

Acknowledgments: CLL thanks Malcolm Sambridge (Seismology & Mathematical Geophysics, RSES, Australian National University), Lexing Xie and Cheng Soon Ong (CECS, Australian National University), and S. K. Lee (Seoul National University) for various discussions regarding optimization, machine learning, and the implementation of the present model. **Funding:** CLL acknowledges funding from a “Chaire d’Excellence” from the Université de Paris, from the Australian Research Council Laureate Fellowship FL1600000 to Prof. Hugh O’Neill (ANU-RSES) as well as from the Postdoctoral Fellowship of the Carnegie Institution for Science during the realisation of this project. **Author contributions:** CLL designed the study, collected the data, performed Raman and viscosity experiments, developed the computer code and drafted the manuscript. DN and BOM helped in the design of the neural network. CLL, BOM and DN performed Raman measurements. All authors contributed to the final version of the manuscript. **Competing interests:** Authors declare no competing interests. **Data and materials availability:** All the data are available in the main text or the supplementary materials. The computer code to reproduce the results of this study is available as a Python library at the web address https://github.com/charlesll/neuravi .

Supplementary Materials:

Materials and Methods

Supplementary Text

Figures S1-S7

Tables S1-S3: Composition of the synthesized glasses.

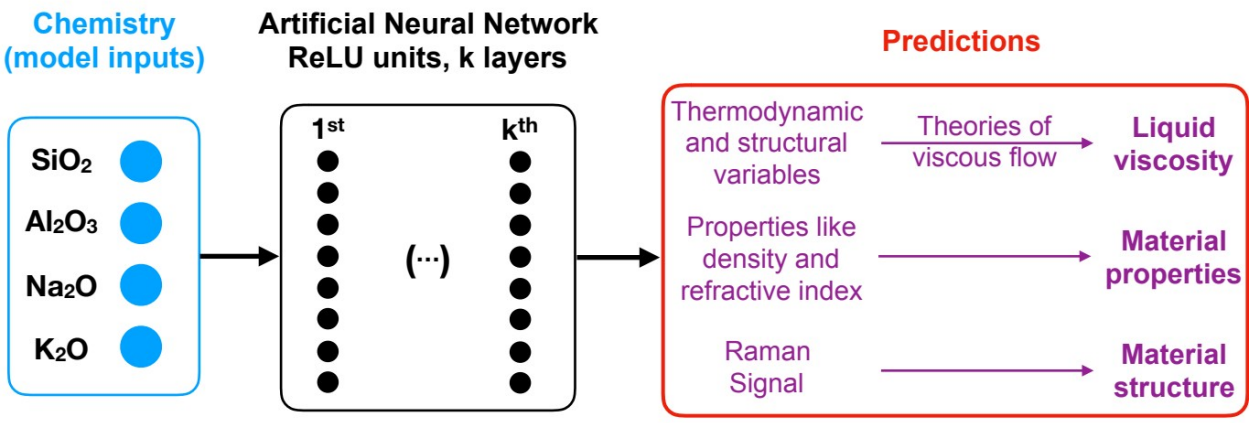

Fig. 1. Presentation of the model. The melt composition is given in input to a deep neural network that predicts various melt and glass properties as well as their Raman vibrational properties (see text for details). Viscosity can then be calculated via different theories, and the relationships between chemistry, structure and properties of the melt and glasses systematically explored using this framework.

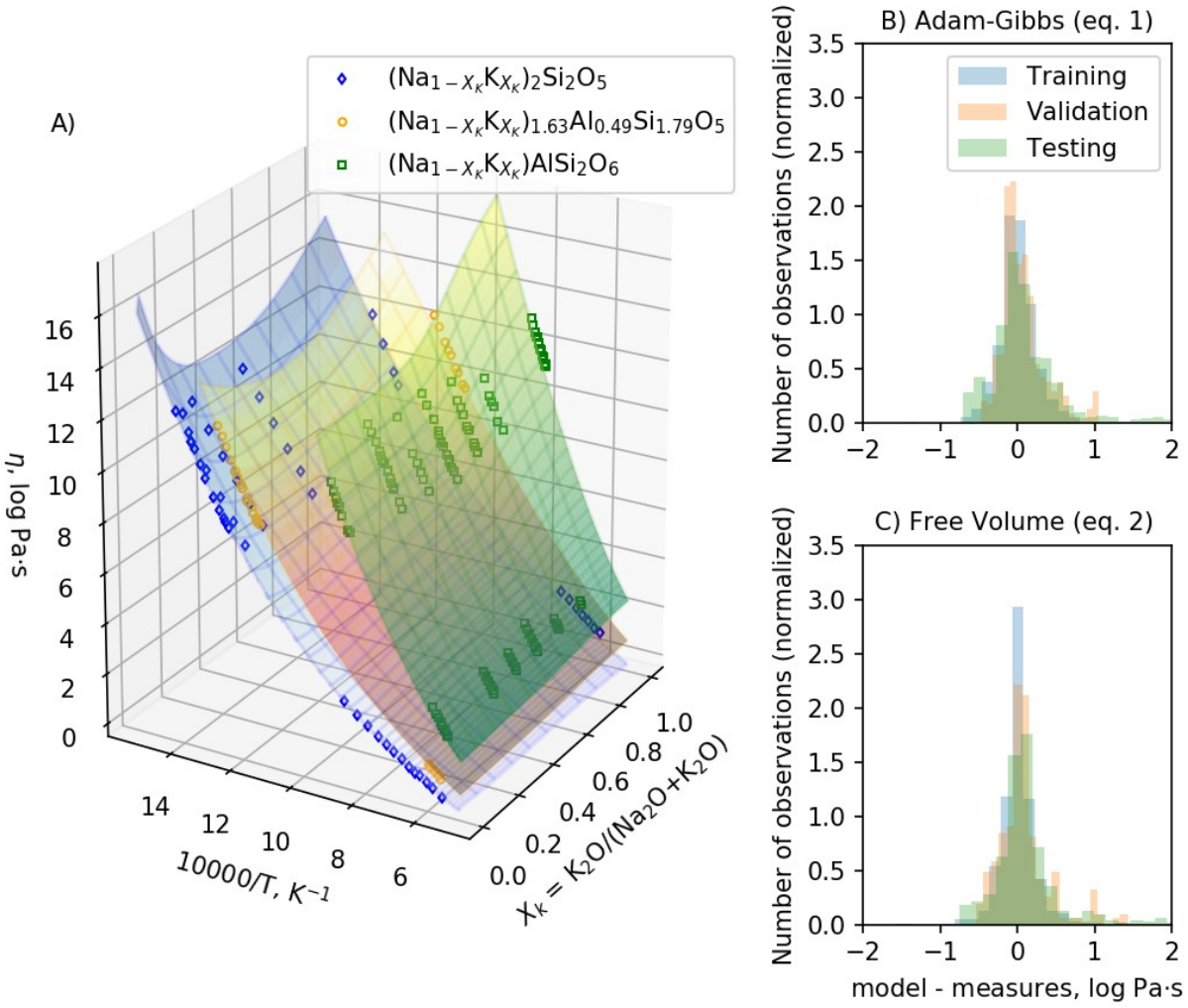

Figure 2: Example of viscosity predictions and observation of viscosity precision. (A) Measurements (symbols) and model predictions using eq. (1) (colored wireframe) are reported as a function of inverse temperature for three different melt series with variable metal to aluminium ratios. (B) and (C) are histograms of the difference between model viscosity predictions using eqs. 1 and 2 and measurements for the different data subsets. See also Table S3 and Figure S3.

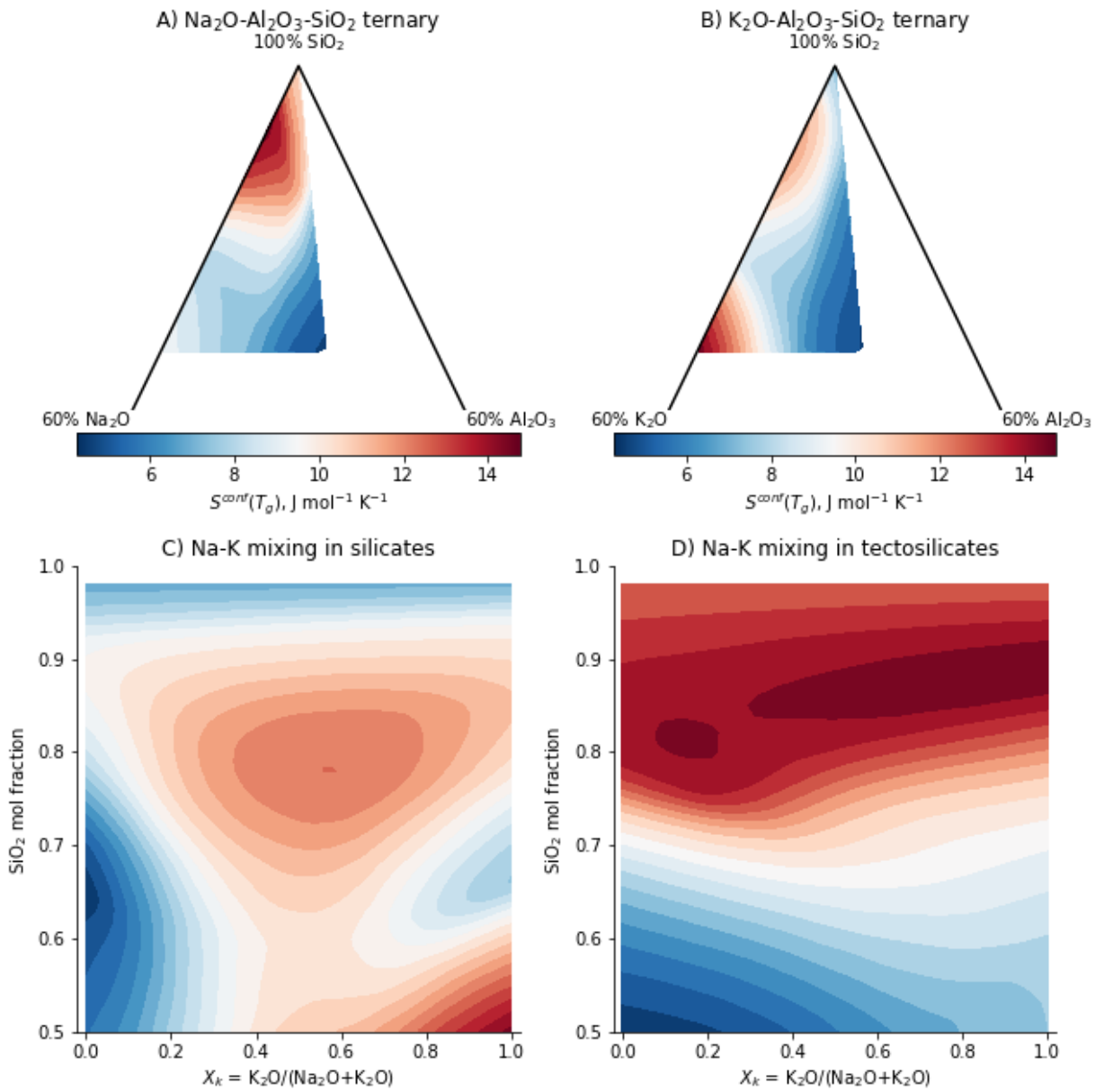

Figure 3: Maps of configurational entropy at the glass transition temperature. $S^{conf}(T_g)$, is shown in the A) sodium and B) potassium aluminosilicate systems as well as during Na-K mixing in C) silicates (no Al) and D) tectosilicates (Al/(Na+K) = 1) compositions. Addition of aluminum generally result in decreasing $S^{conf}(T_g)$, which reach minimal values close to the *nepheline-orthoclase* composition. During Na-K mixing, excess entropy appears when those elements are network modifiers (in silicate, C) but is not detected in Al-rich compositions (e.g. in aluminosilicates, D).

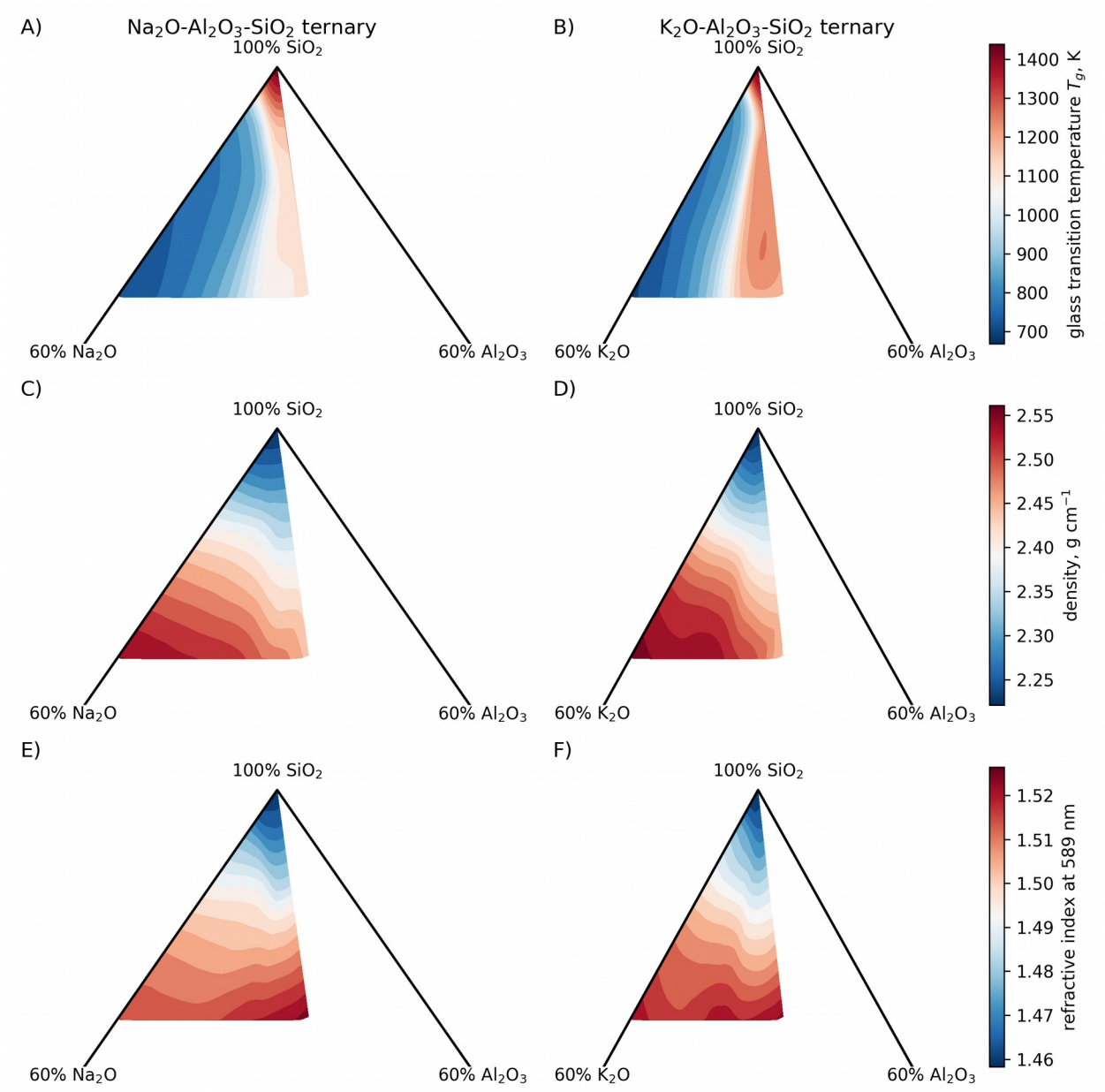

Figure 4: Maps of glass transition temperature, glass density and glass refractive index. Glass transition temperature varies strongly with the (Na+K)/Al ratio and silica content in both the sodium (A) and potassium (B) aluminosilicate systems, while glass density (C, D) or optical refractive index depend mostly on the glass silica content (E, F).

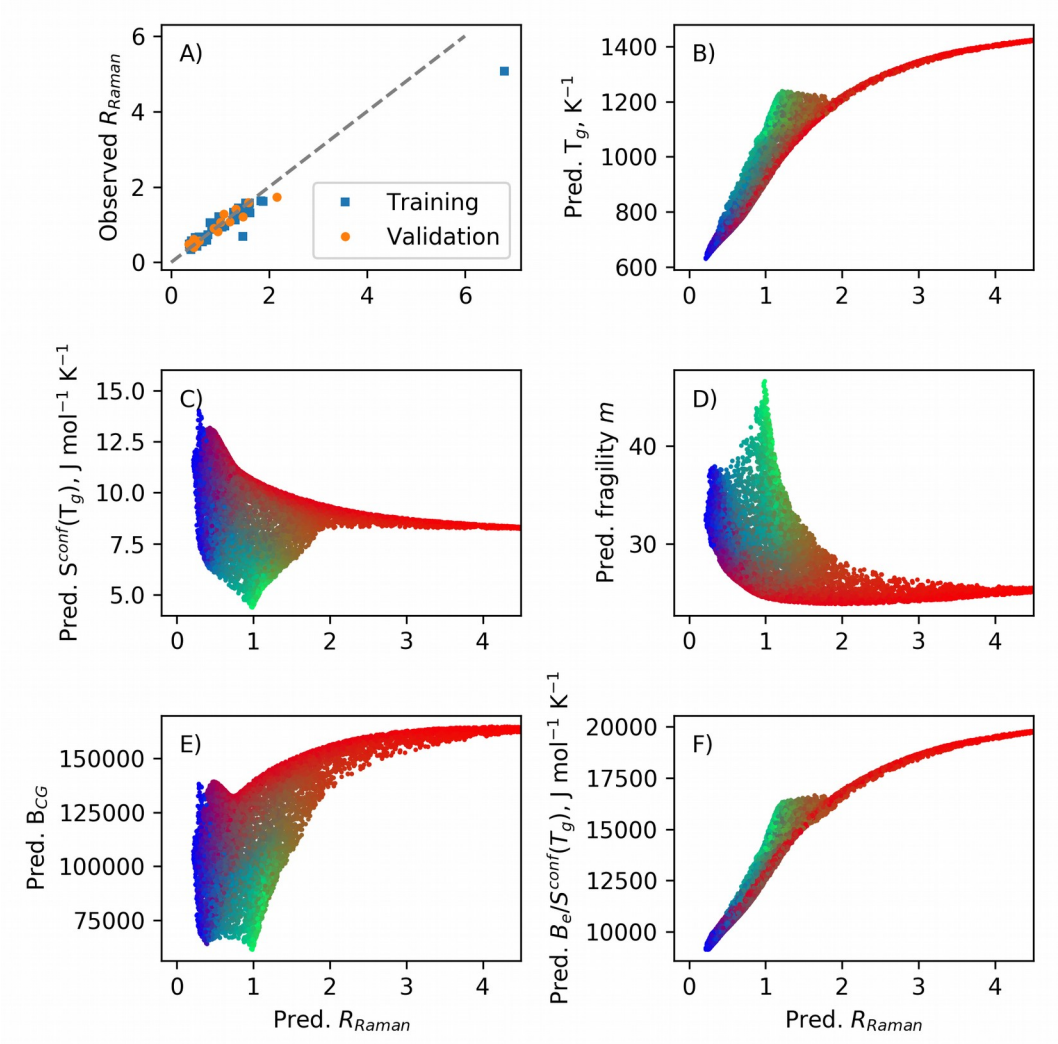

Figure 5: Relationship between glass Raman spectra and glass properties. The ratio of the intratetrahedral to intertetrahedral vibrations, R_{Raman} (see text for explanation), is a proxy for network topology. It is well reproduced by the present model despite a limited training set (A); the model thus captured well how glass composition is linked to their Raman signal and thus structure. R_{Raman} correlates well with T_g (B) or $B_e/S^{conf}(T_g)$ (F), but variations with $S^{conf}(T_g)$, m or B_{CG} are of a more complex nature (C, D, E). Each point is part of 10,000 randomly generated compositions in the quaternary diagram. Symbol colors are in RGB format and embed compositional information as red is scaled mol fraction of SiO_2, green is scaled mol fraction of Al_2O_3, and blue is scaled mol fraction of K_2O+Na_2O. This allows to observe a clear compositional mapping in variations of $S^{conf}(T_g)$, m or B_{CG}.